Gravity and Magnetic Investigation of the Surtsey Volcano

of

Iceland’s Vestmannaeyjar Archipelago

Senior Thesis
Submitted in partial fulfillment of the requirements for the
Bachelor of Science Degree
At The Ohio State University

By
Stas Sudilovsky

The Ohio State University
2018

Approved by:

____

Ralph R.B. von Frese

Academy Professor

School of Earth Sciences

Table of Contents

ABSTRACT

This study integrated topography, and anomalous gravity and magnetic data for the crustal attributes of the juvenile Surtsey volcano, which is part of the Vestmannaeyjar archipelago off the southern tip of Iceland on the Atlantic Ridge. Crustal models that jointly satisfy multiple datasets typically are more reliable than one based only on a single set of data. Here, the modeling used Geosoft's Oasis montage software to access and process the datasets. The modeling suggested that Surtsey's subsurface architecture is much more extensive than its terrestrial edifice. It also constrained crustal temperature variations that inverse gravity and magnetic anomaly correlations may flag. Enhanced heat depresses crustal magnetization and its magnetic anomaly and increases the related gravity anomaly due to the inflation of the crust and its density contrast relative to the overlying air/sea water environment and vice versa. Geothermal modeling MatLab code also was developed to suggest that Surtsey might achieve thermal equilibrium on the scale of some 10^5 yrs. These results provide a template for considering the crustal properties of the other volcanoes of the Vestmannaeyjar archipelago that sits on a propagating oceanic ridge.

ACKNOWLEDGEMENTS

I thank my research advisor Dr. Ralph von Frese for his patience and advice in support of my project. I also thank Dr. Carey for always being there and willing to help. In addition, I thank Dr. Sawyer, for helping to advise me on further educational and professional opportunities, and supporting the presentation of some of my results at The Ohio State University as part of the Shell Undergraduate Research Experience (SURE) program. SURE program funding from the Shell Exploration and Production Company partially supported my research. I also thank my Earth Science's professors for providing productive classroom and extracurricular experiences. Finally, I thank my family and friends for their support during my education that allowed me to overcome difficulties and accomplish my academic objectives.

List of Figures

INTRODUCTION

Volcanoes are dynamic structures involving moving and mixing magma beneath the Earth's surface driven by crustal temperature differences (e.g., Duffield et al., 1975). This study uses gravity and magnetic anomaly data to investigate the crustal architecture of the Surtsey volcano, which began erupting above sea level in 1963 offshore of Iceland's southeastern coast (Figures 1 & 2). It is forming in the East Volcanic zone of the propagating Mid-Atlantic ridge as part of the Vestmannaeyjar archipelago (e.g., Moore., 1992).

The crustal model developed from publicly available gravity and magnetic data archives was also used in combination with borehole geothermal measurements to constrain the timescale for Surtsey to reach thermal equilibrium. The analysis used Fourier's law to extend Surtsey's thermal properties from the initial eruption into the future. Accordingly, the results of this study provide a template for the crustal architecture and thermal attributes of other newly formed volcanoes of the Vestmannaeyjar archipelago.

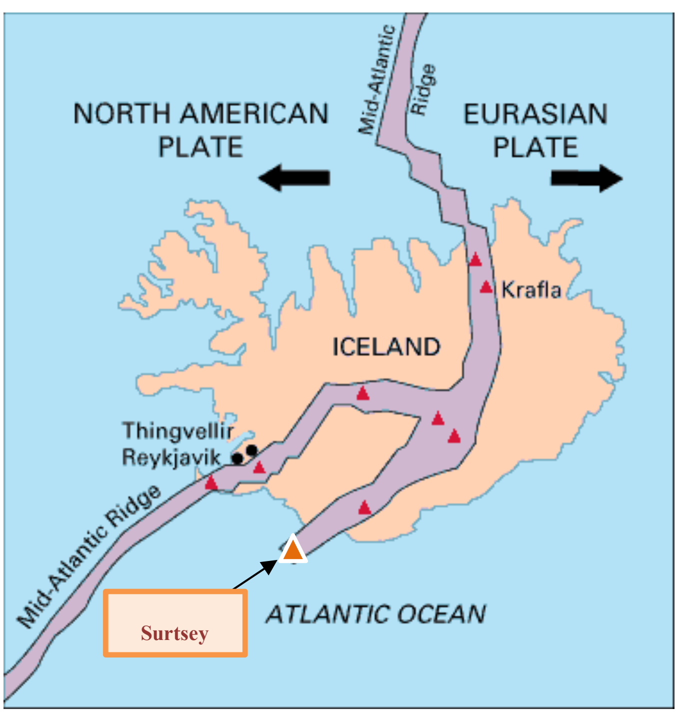

Figure 1. Location of Iceland's Surtsey volcano on the eastern limb of the Mid-Atlantic ridge.

Figure 2. Aerial view of Surtsey and other islands of the Vestmannaeyjar archipelago (https://earthexplorer.usgs.gov/).

METHODS

For this study, the US Geological Survey's GTOPO30 model (https://earthexplorer.usgs.gov/) provided bathymetry data consisting of 30 arc second topographic elevation averages for the area 62.8°N –63.8°N and 20°W –21°W at the grid interval of 1 km. The Bureau Gravimétrique International (BGI) database (http://bgi.omp.obs-mip.fr/data-products/Gravity-Databases) provided gridded free-air gravity anomaly (FAGA) data for the region. In addition, Oasis Montaj's "seek data" option extracted magnetic total field anomaly values from the Geological Survey of Canada's (GSC) archive for the gridded region. GEOSOFT's Oasis Montaj (OM) software produced high-resolution maps of the bathymetry (Figure 3), free-air gravity anomaly (Figure 4), and total field magnetic anomaly (Figure 5) data using the WGS'84 UTM zone 27N projection.

The GTOPO30 topographic elevations, BGI free-air gravity, and GSC magnetic total field anomalies were freely downloaded as ASCII files for OM processing. Both the gravity and magnetic data were gridded at sea level. Each of the ASCII files was uploaded into the project database, where the map's coordinate projection, contour interval and color bar were specified. Next, a common base map for the study region was defined onto which each data grid was projected. OM's data seeker function also was used to download the island shorelines for the base map plots.OM also provides an option to obtain key profiles from the gridded data for more detailed crustal analysis. Examples include the A-A' and B-B' profiles across the respective Surtsey and Heimaey volcanoes in Figures 3, 4, and 5. Figure 6 gives the ASCII values for the three datasets extracted for the B–B' profile by OM's profiler option, whereas Figure 7 compares the profiled data plots.

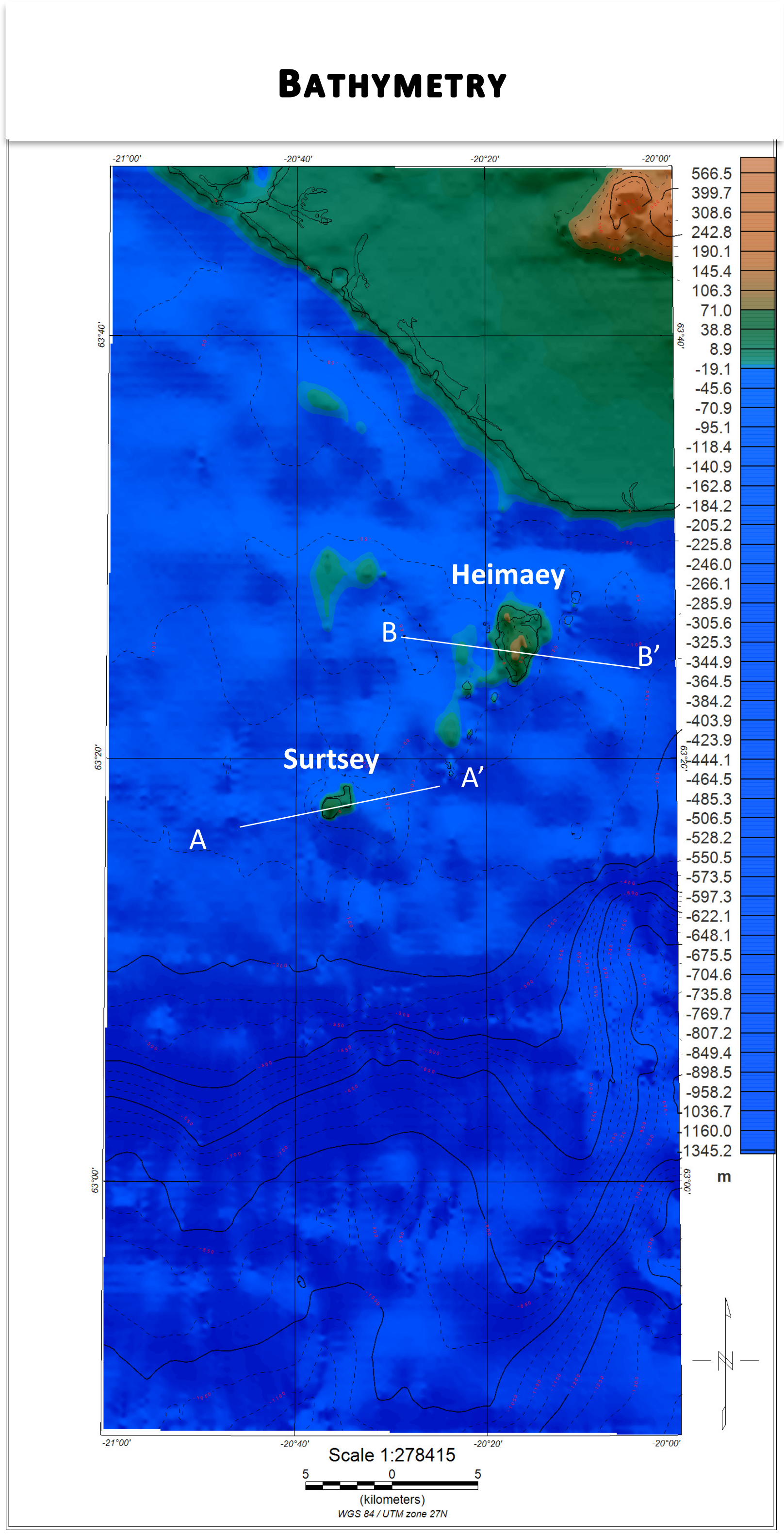

Figure 3. Bathymetry map for the Surtsey study area showing profiles A-A’ and B-B’ that were analyzed for crustal properties in this study.

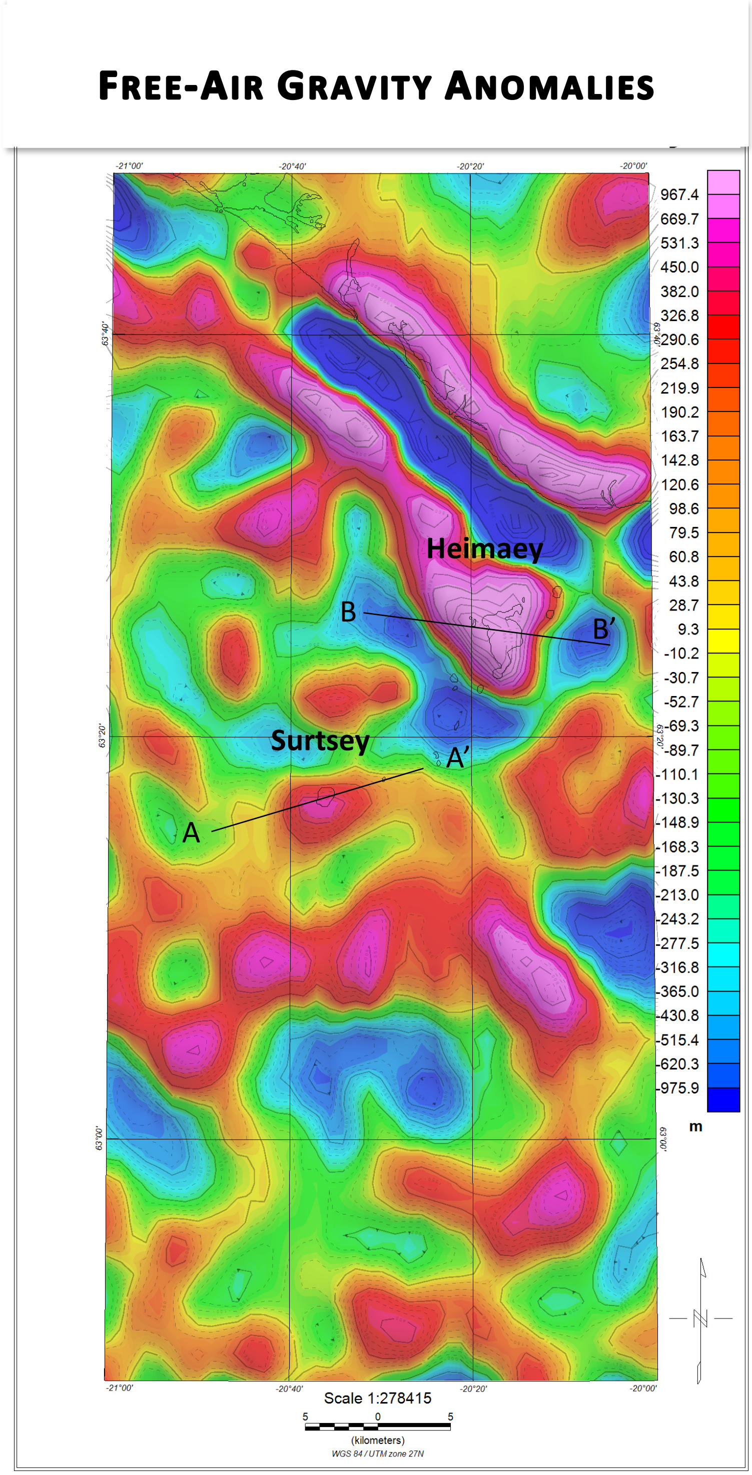

Figure 4. Free-air gravity anomaly map of the Surtsey study area showing profiles A-A' and B-B' that were analyzed for crustal properties in this study.

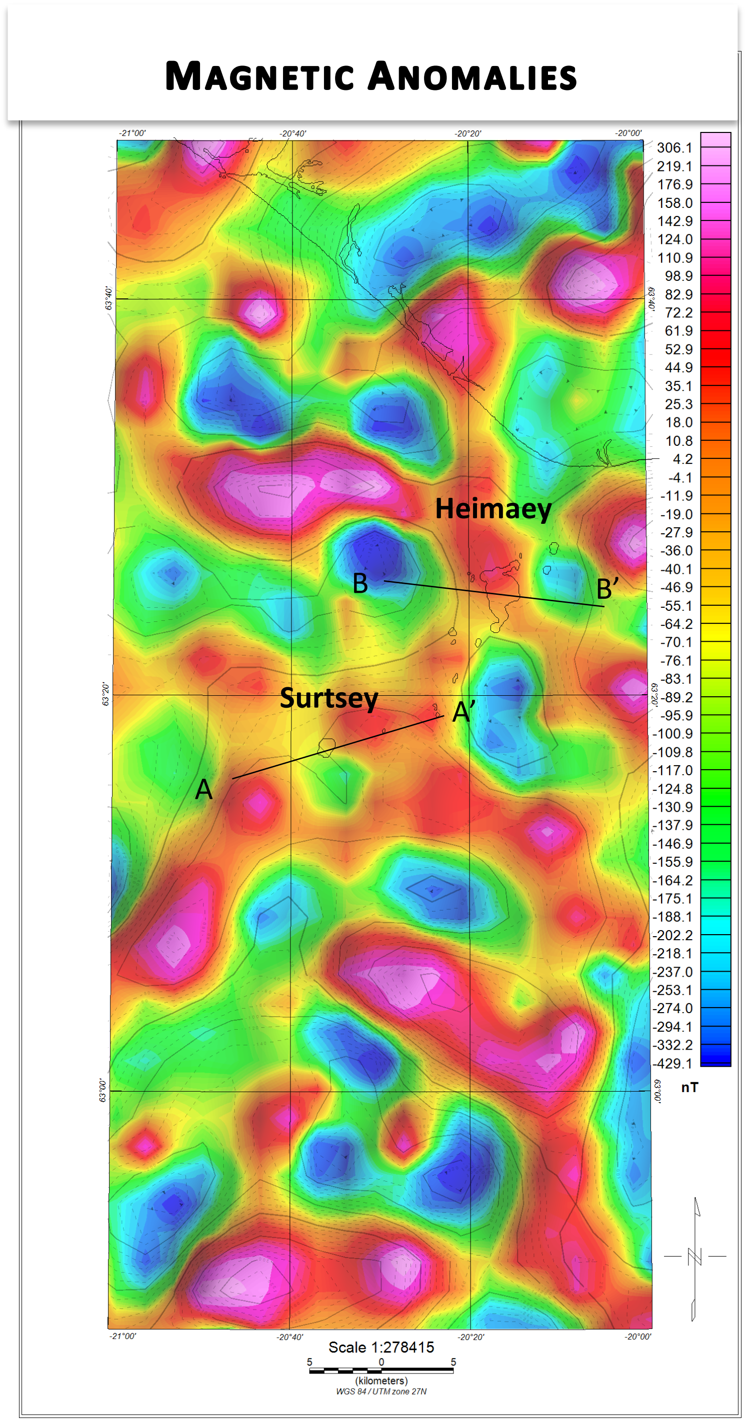

Figure 5. Magnetic total field anomalies of the Surtsey study area showing the profiles A-A' and B-B' that were analyzed for crustal properties in this study.

✔ S1:0	X x	Y y	Bathymetry	Gravity	Magnetics
0.0	525.7	7032.7	-38.1	-6.7	-7.3
1.0	525.8	7032.7	-41.3	-6.8	-9.2
2.0	526.0	7032.7	-44.8	-6.6	-12.3
3.0	526.1	7032.7	-48.2	-6.4	-14.4
4.0	526.3	7032.7	-51.1	-6.3	-17.7
5.0	526.4	7032.7	-53.4	-6.1	-20.0
6.0	526.6	7032.7	-55.5	-6.2	-23.5
7.0	526.7	7032.7	-57.2	-6.1	-26.1
8.0	526.9	7032.7	-58.4	-6.0	-29.7
9.0	527.1	7032.7	-59.1	-5.8	-32.5
10.0	527.2	7032.7	-59.3	-5.9	-35.3
11.0	527.4	7032.7	-59.3	-5.8	-39.3
12.0	527.5	7032.7	-59.2	-5.8	-42.4
13.0	527.7	7032.7	-58.6	-5.7	-46.6
14.0	527.8	7032.7	-57.4	-5.8	-47.8
15.0	528.0	7032.7	-56.0	-5.8	-47.5
16.0	528.2	7032.7	-54.6	-5.8	-46.1
17.0	528.3	7032.7	-53.1	-5.8	-44.5
18.0	528.5	7032.7	-51.3	-5.9	-43.9
19.0	528.6	7032.7	-49.3	-5.7	-42.2
20.0	528.8	7032.7	-47.2	-5.6	-41.3
21.0	528.9	7032.7	-44.9	-5.4	-39.4
22.0	529.1	7032.7	-41.9	-5.3	-38.3

Figure 6. ASCII values extracted for the B-B' profiles across Heimaey. The first column gives the station identifiers. The next two columns hold the data coordinates in km, and the last three columns hold the data in units of m, mGal, and nT, respectively.

The data extracted for the A–A' profile across Surtsey are shown in the crustal modeling results of Figure 8 that were obtained using OM's Gm-SYS 2D modeling option. In particular, the solid black lines in the top two panels of Figure 8 show the extracted anomalous magnetic and gravity data, respectively, whereas the red dotted line in the bottom panel gives the extracted bathymetric and terrestrial elevations.

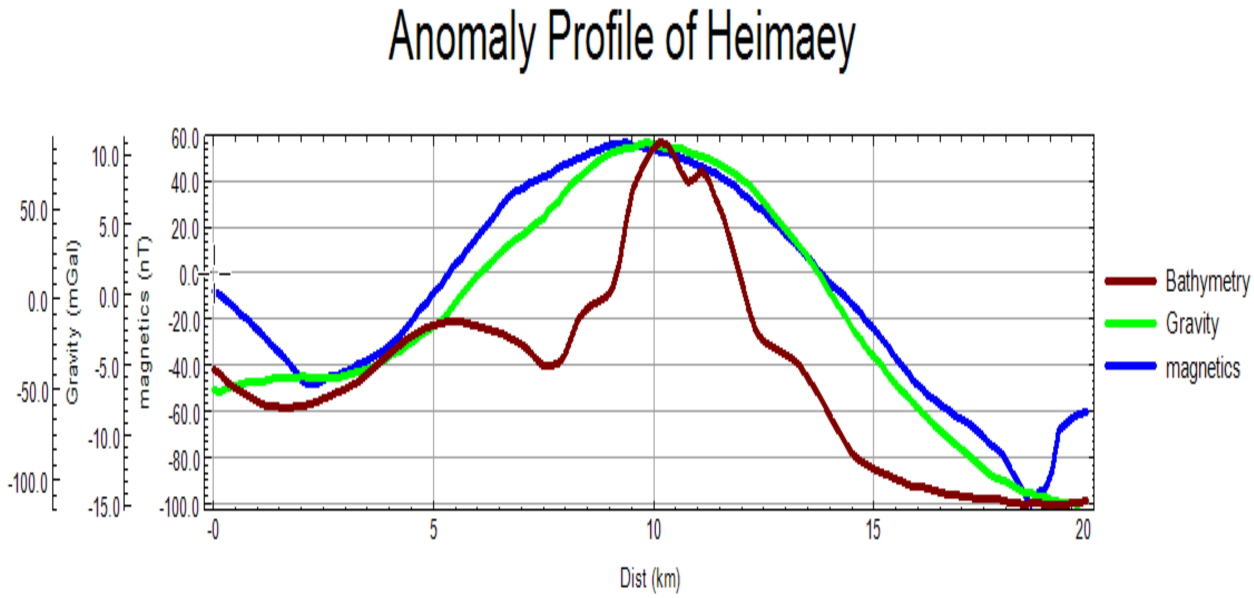

Figure 7. Data comparisons along profile B (left)–B' (right). Each profile includes 127 values at an interval of 0.16 km. The gravity and magnetic data are at sea level, and the bathymetry data are relative to sea level in m.

The bottom panel (Figure 8) also shows the crustal cross-section of magnetic susceptibility and density contrasts with effects given by the black dotted profiles that approximately fit the respective observed magnetic and gravity anomaly data (solid black profiles) in the top two panels. Interactive graphical construction of the 7 crustal polygons by trial-and-error inferred the crustal distribution of the physical property variations in the bottom panel. The crustal polygons include Surtsey's above sea level tephra edifice (brown colored), sea water component (blue colored), oceanic sedimentary section (green colored), the upper (Body 1) and lower (Body 2) components of the magma chamber, hotter oceanic crust (Body 3) underlying the magma chamber, and normal oceanic crust (Body 4).

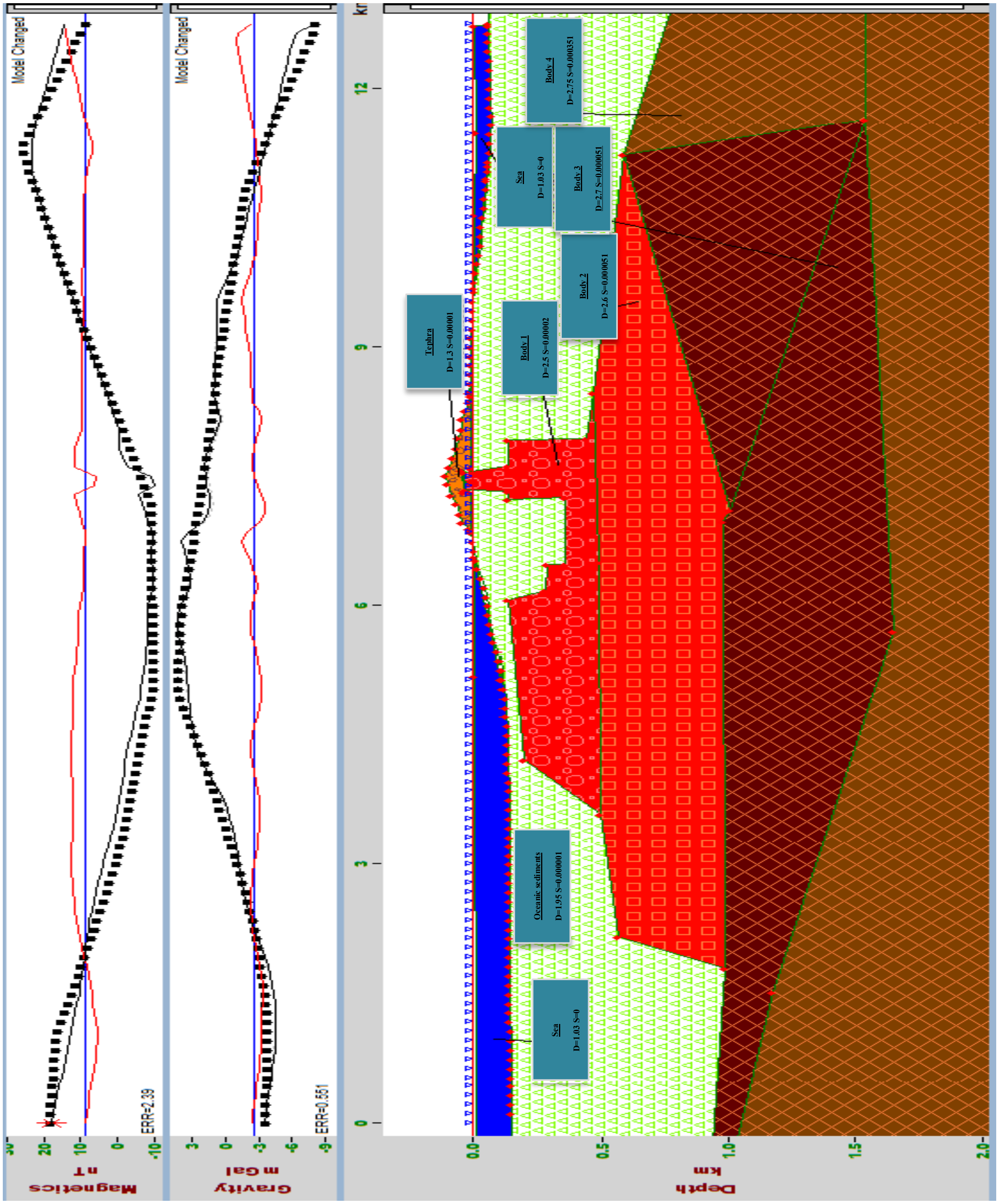

Figure 8. GmSYS crustal modeling (bottom panel) of anomalous magnetic (top panel) and gravity (middle panel) data of the A(SW)-A'(NE) profile across Surtsey subject to the crustal section's 30 arc minute bathymetric and terrain elevation (i.e., topographic) constraints (red dotted profile).

Published physical property tables of the materials (e.g., Sangode et al., 2017) provided the magnetic susceptibility and density estimates used for computing the respective magnetic and gravity effects of the polygons. In the top two panels, the black dotted profiles show that these modeled effects fit the A-A' profile anomalies very well to within the errors given by the solid red lines.

The crustal modeling provided an opportunity to explore the cooling rate of the inferred magma chamber using the available magnetic constraints. This assessment is possible because rock magnetization depends on the Currie temperature at which the magnetization is lost (e.g., Dzurisin et al., 1990). Thus, following Dzurisin et al. (1990) and Turcotte & Schubert (2004), Fourier's law was used to estimate the time required for the crustal model to reach temperature equilibrium. Simplifying assumptions precluded the injection of new magma into the chamber, heat production by radioactive decay, seasonal temperature variations, and the penetration of ocean water into the crust.

The thermal modeling synthesized the inferred igneous crustal components in Figure 8 into the four 2-D bodies presented in Figure 9. Here, the main rock type assumed is basaltic in composition with the generalized magnetic susceptibility versus temperature variations shown in Figure 10, which provided the initial approximate temperature estimates in Figure 9 as drawn from the crustal modeling of the magnetic, gravity, and topography data in Figure 8.

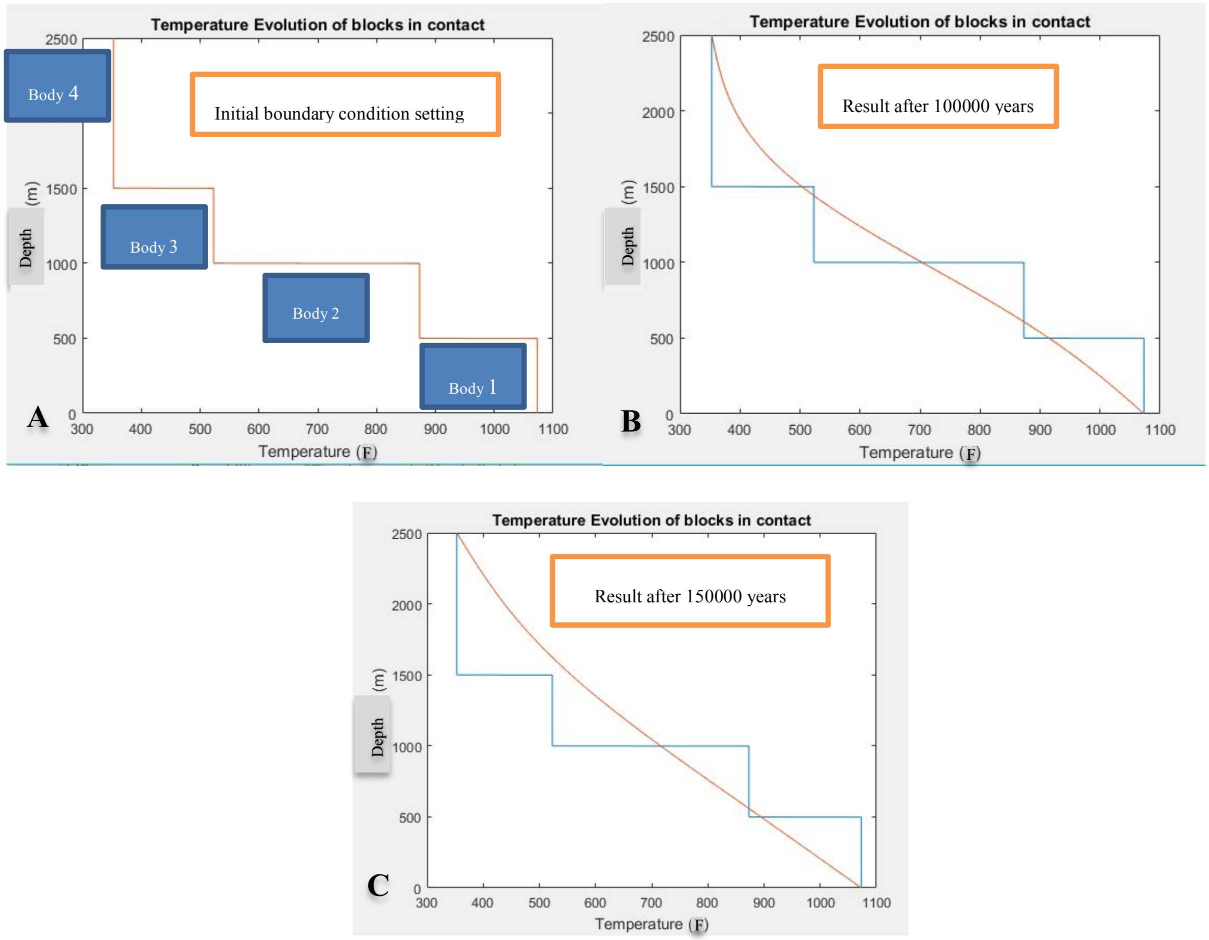

Figure 9. Modeling the cooling rate of Surtsey's inferred igneous crust in Figure 8.

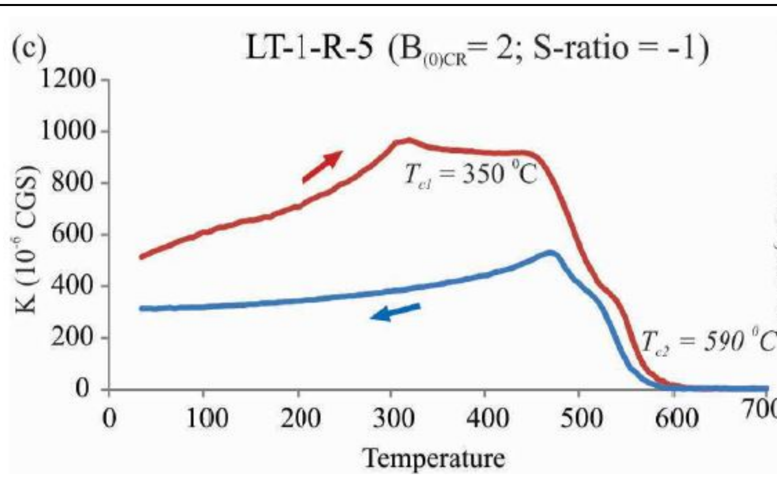

Figure 10. Magnetic susceptibility versus temperature curve for basalt (Sangode et al., 2017) used to set the initial temperatures in Figure 9 for estimating the thermal equilibrium of Surtsey's igneous crustal model in Figure 8.

Accordingly, Figure 9 represents Body 1 with the thickness of 0.5 km and average initial temperature T = 353°F (178°C), Body 2 of thickness 0.5 km and T = 523°F (272°C), Body 3 of thickness 0.5 km and T = 873°F (467°C), and Body 4 of thickness 1.0 km and T = 1073°F (578°C). The analysis numerically estimated the time it takes to linearize the temperature equation over depth x (in m) for tabular bodies with large horizontal dimensions compared to x (e.g., Turcotte & Schubert, 2014) given by

$$T(t_0 + \Delta t) = T(t_0, x_0) + \Delta t \frac{k}{\delta x^2} \left(T(x + \delta x, t_0) + T(x - \delta x, t_0) - 2T(x, t_0)\right),$$

where T is temperature (in °F), t_0 is initial time (in sec), Δt is the time step interval (in sec), δx is the depth step interval (in m), and k is the thermal diffusivity (in m^2/sec).

In addition, the analysis assumed that all the bodies were basalt with uniform $k = 10^{-6}$ m^2/sec, and the time step was 2-weeks or Δt = 1,209,600 sec**.** This time step was appropriate because it is small relative to realistic cooling rates of the order of 10^5 years, but also large enough to limit extraneous computations. The best cooling rate estimate is the period of time required for the above equation to linearly fit the initial temperature data of Figure 9**.**

RESULTS

OM's plotting tools processed the uploaded ASCII values of the grids covering the Vestmenajyaer archipelago into maps. The maps included the 30 arc minute bathymetry and terrestrial elevation data from the GTOPO30 model (Figure 3), the free-air gravity anomaly data extracted from the Bureau Gravimétrique (Figure 4), and the magnetic anomaly data imported from the GSC archive (Figure 5). All maps include a legend, north arrow, scale, color bar with the amplitude units, and the outlines of the landmasses for geographic reference.

The maps also show the A-A' and B-B' traverses across the respective Surtsey and Heimaey volcanoes, which are further considered in Figures 8 and 7, respectively. The traverses include 3 datasets each of 127 values at an interval of 0.16 km. The positively and negatively correlated gravity and magnetic anomalies across Heimaey (Figure 7) and Surtsey (Figure 8), respectively, are consistent with younger and thus significantly hotter crust hosting the Surtsey volcano. The bottom panel of Figure 8 also shows possible distributions of density and magnetic susceptibility variations that yield effects which closely approximate the gravity and magnetic anomalies of the A-A' traverse.

To evaluate the thermal equilibrium of the igneous components of Surtsey's inferred crust in Figure 8, the simplified thermal model consisting of the 4 temperature differentiated 2-D bodies in Figure 9 was considered. Following Aboud et al. (2015), the bodies were assumed to be mainly basalt at initial temperatures set by Figure 10. Figure 9 also includes the results for running the above equation over terminating periods of 100 Kyrs (upper right panel) and 150 Kyrs (lower middle panel). The 150-Kyr period yields the best linear fit, and thus it is an acceptable estimate of the thermal equilibrium period. Over shorter periods, the equation predicts higher order polynomial approximations, whereas at longer periods the fits become increasingly higher frequency and unstable.

Figure 11 shows the borehole lithologies and temperature changes over a period of 30 years for Surtsey's upper ~180 m. They provide important constraints on the crustal and thermal modeling of Surtsey. For example, the temperature of the 1st body was assumed to have temperature contribution from the above sea level terrestrial body, which increased the initial stated temperature for the computational model.

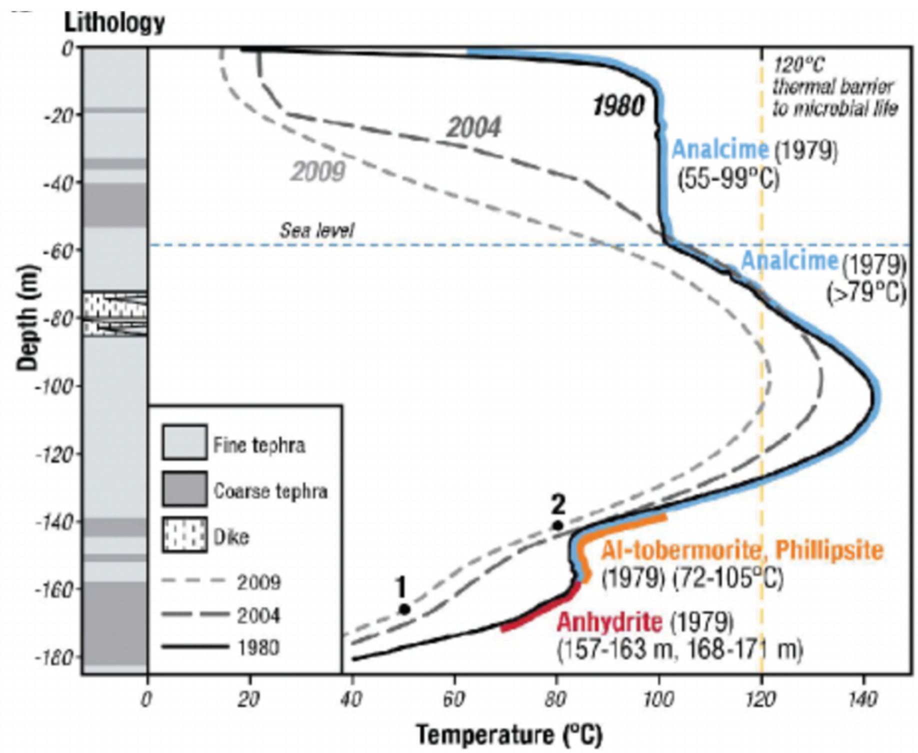

Figure 11. Borehole measurements showing the lithologies and temperature changes over a 30-year period in the upper ~180 m of the Surtsey volcano (Jackson et al., 2015).

Discussion

The gravity anomaly over Heimaey is about 400 mGal stronger than that of Surtsey and correlates positively with the size of the islands (Figure 4).. The larger the island, the larger is its density difference relative to that of its country air and sea water environment. However, the anomalies are not centered on the islands, suggesting that the volcanoes are offset from the main crustal sources of the anomalies.

Other interesting features include the strong negative gravity anomalies reaching minima of about -900 mGal around Heimaey that are more subtly expressed around Surtsey. These anomaly minima may reflect mass deficiency effects related to thinning of the oceanic crust. Similarly, the strong positive gravity anomaly along Iceland's southern coastline may mark the transition into thicker crust.

Figure 5 shows positive magnetic anomalies over Heimaey and relatively negative anomalies over Surtsey. The relative disparity in these amplitudes may reflect a crustal thermal environment for Surtsey that is significantly hotter than that of the Heimaey volcano. Surtsey also has lost half of its land mass due to erosion since its formation (Jakobsson et al., 2000), which has significantly degraded the thermoremanent component of its crustal magnetic signature. At Heimaey, the positive magnetic anomaly mostly overlies the eruption cones on the northern side of the island. In Figures 3, 4, and 5, the profiles A-A' and B-B' were taken along W-to-E traverses. Figure 7 illustrates the positive correlation in the three datasets for Heimaey, whereas Figure 8 shows the inverse correlation between the magnetic anomaly and both the gravity anomaly and bathymetry data.

Figure 8 illustrates the use of OM's Gm-SYS gravity and magnetic anomaly modeling software to develop crustal distributions of density and magnetic susceptibility variations that accommodate the A(W)-A'(E) datasets. The crustal section from about 150 m above sea level to a depth of 2 km is modeled in the bottom panel where the dotted red line represents the bathymetric and terrestrial elevation components of the crustal topography. The top and middle panels show the respective A-A' magnetic and gravity anomaly data (solid black lines), along with their modeled approximations (dotted black lines) and related approximation errors (solid red lines).

The crustal model of density and magnetic susceptibility variations in the bottom panel simplify the crust in terms of 7 layered 2-D sources. The crustal modeling suggests that a much more extensive magma chamber underlies Surtsey as a principal source contributing to the magnetic and gravity anomaly observations. In general, the archipelago is located along a propagating ridge that began opening at ca. 20 Myrs (Mattsson & Hoskuldsson ,2003), fed by a hot spot at a depth of approximately 10 km below sea level (Thy, 1991).

The simplified crustal model also facilitates estimating an equilibrium temperature for Surtsey by assuming initial temperatures for each body. However, the assumed temperatures are only approximations due to the uncertainties concerning the mineralogical variations and their effects on susceptibility**.** Furthermore, the analysis assumed a constant value of heat diffusivity for all the bodies, although slight variations are possible due to the basaltic rock chemistry differences at the various temperatures.

The best linear fit to the initial temperature distribution is in the bottom panel of Figure 9C, which suggests a thermal equilibrium period of roughly 150 Kyrs for Surtsey's crust. Shorter periods yield distinct low-order polynomial fits as shown in the upper right panel, whereas longer periods yield unstable, high-order polynomial fits. Additional seismic surveying and drilling can resolve further details concerning Surtsey's crustal properties to reduce thermal modeling errors.

Conclusions and Recommendations

Modeling of combined data of terrain elevation, magnetic, and gravity imply 7 possible magnetic susceptibility and density variations of Surtsey's crustal environment. The inverse anomaly correlation of a gravity maximum and magnetic minimum over Surtsey contrasts with the direct correlation of anomaly maxima over Heimaey to suggest that significantly hotter crust hosts the younger Surtsey volcano. Simplified thermal analysis of Surtsey's current igneous upper 2-km crustal model suggests that it may achieve thermal equilibrium in approximately 150 Kyrs.

In general, the crustal and thermal models of this study provide templates for investigating other volcanoes of the Vestmannaeyjar archipelago, as well as newly forming volcanoes on any propagating oceanic ridge. However, care must be taken with these results because they are not unique and subject to errors in the data and modeling assumptions. Additional crustal drilling and geophysical studies including seismic surveying can greatly limit these modeling uncertainties.

References Cited

Aboud, E., El-Masry, N., Qaddah, A., Alqahtani, F., and Moufti, M.R., 2015, Magnetic and gravity data analysis of Rahat Volcanic Field, El-Madinah city, Saudi Arabia: NRIAG Journal of Astronomy and Geophysics, v. 4, p. 154–162, doi: 10.1016/j.nrjag.2015.06.006.

Omp BGI: Bureau Gravimétrique International, http://bgi.omp.obs-mip.fr/ (accessed June 2017).

Duffield, Wendell A, 1975, Structure and origin of the Koae fault system, Kilauea Volcano, Hawaii; U.S. Geological Survey Professional Paper No. 856.

Dzurisin, D., Denlinger, R.P., and Rosenbaum, J.G., 1990, Cooling rate and thermal structure determined from progressive magnetization of the Dacite Dome at Mount St. Helens, Washington: Journal of Geophysical Research, v. 95, p. 2763, doi: 10.1029/jb095ib03p02763.

Jackson, M.D., Gudmundsson, M.T., Bach, W., Cappelletti, P., Coleman, N.J., Ivarsson, M., Jónasson, K., Jørgensen, S.L., Marteinsson, V., Mcphie, J., Moore, J.G., Nielson, D., Rhodes, J.M., Rispoli, C., et al., 2015, Time-lapse characterization of hydrothermal seawater and microbial interactions with basaltic tephra at Surtsey Volcano: Scientific Drilling, v. 20, p. 51–58, doi: 10.5194/sd-20-51-2015.

Jackson, M.D., Gudmundsson, M.T., Bach, W., Cappelletti, P., Coleman, N.J., Ivarsson, M., Jónasson, K., Jørgensen, S.L., Marteinsson, V., Mcphie, J., Moore, J.G., Nielson, D., Rhodes, J.M., Rispoli, C., et al., 2015, Time-lapse characterization of hydrothermal seawater and microbial interactions with basaltic tephra at Surtsey Volcano: Scientific Drilling, v. 20, p. 51–58, doi: 10.5194/sd-20-51-2015.

Mattsson, H., and Höskuldsson, Á., 2003, Geology of the Heimaey volcanic centre, south Iceland: early evolution of a central volcano in a propagating rift?: Journal of Volcanology and Geothermal Research, v. 127, p. 55–71, doi: 10.1016/s0377-0273(03)00178-1.

Moore, J.G., Jakobsson, S., and Holmjarn, J., 1992, Subsidence of Surtsey volcano, 1967?1991: Bulletin of Volcanology, v. 55, p. 17–24, doi: 10.1007/bf00301116.

NOAA National Centers for Environmental Information (NCEI): NOAA National Centers for Environmental Information (NCEI), https://ngdc.noaa.gov/ (accessed June 2017).

Sangode, S.J., Sharma, R., Mahajan, R., Basavaiah, N., Srivastava, P., Gudadhe, S.S., Meshram, D.C., and Venkateshwarulu, M., 2017, Anisotropy of magnetic susceptibility and rock magnetic applications in the Deccan volcanic province based on some case studies: Journal of the Geological Society of India, v. 89, p. 631–642, doi: 10.1007/s12594-017-0672-1.

Thy, P., 1991, High and low pressure phase equilibria of a mildly alkalic lava from the 1965 Surtsey eruption: Experimental results: Lithos, v. 26, p. 223–243, doi: 10.1016/0024-4937(91)90030-o.

Turcotte, D., and G. Schubert, *Geodynamics (3rd Ed.)*, Cambridge University Press, 2014; 636 pages.